

Backward-motion control of a mobile robot with n passive off-hooked trailers[†]

Woojin Chung^{1,*}, Myoungkuk Park², Kwanghyun Yoo¹, Jae Il Roh¹ and Jongsuk Choi³

¹School of Mechanical Engineering, Korea University, Seoul, 136-701, Korea

²Department of Mechanical Engineering, Texas A&M University, Texas 77840, U.S.A.

³Korea Institute of Science and Technology, Seoul, 136-791, Korea

(Manuscript Received June 14, 2010; Revised October 26, 2010; Accepted July 27, 2011)

Abstract

A passive multiple-trailer system provides various practical advantages for multi-functional service robots. However, motion control is difficult because the kinematic model is highly nonlinear. The kinematic design of a trailer system was proposed in prior research of ours. In this paper, it is shown how the backward motion of a robot with n passive trailers can be controlled. Once the desired trajectory of the last trailer is computed, the control input of the pushing robot is obtained through the proposed control scheme. Some experimental issues on reversing the trailer system are addressed. This paper provides an answer to the following question: "Does the system work well even if there are sensing or modeling errors?" Although it is difficult to obtain general analytic solutions for the above research question, a practical answer will be explored through simplified analysis and experiments. Experimental verifications are carried out using a mobile robot with three passive trailers. The experimental results show that backward-motion control can be successfully carried out by applying the proposed control scheme.

Keywords: Passive trailer; Reconfigurable robot; Backward-motion control; Trajectory tracking; Under-actuated system

1. Introduction

Passive trailer systems provide various practical advantages for multi-functional service robots. One example of a multi-functional service robot was introduced in our prior research [1]. The costs of fabrication and operation of passive trailers are lower than the cost of using multiple autonomous mobile robots. A robot can achieve reconfigurability and extensibility by using modular trailers. Mobile robots are receiving considerable attention as shown in recent publications [2-4].

The major drawback of multi-body passive trailers is the difficulty of motion control. The kinematic model is represented by highly nonlinear equations. There are two velocity inputs and $n+3$ generalized coordinates, which implies that the trailer system is an under-actuated system. The reversing of trailers is an open-loop unstable control problem. More specifically, pushing three or more trailers is extremely difficult in practical applications, as explained in Ref. [5].

So far, trailer systems have received considerable attention from the viewpoint of nonlinear control theory. Laumond [6] showed the controllability of a multiple-trailer system. In Ref. [7], Murray and Sastry proposed a chained form.

A class of multiple-trailer systems can be easily controlled by exploiting the chained form conversion. Typical examples are the open loop-strategies proposed by Tilbury, Murray, and Sastry in Ref. [8] and the closed-loop controller of Sørdalen and Wichlund in Ref. [9]. In Ref. [10], Rouchon et al. proposed an open loop motion-generation strategy that uses differential flatness. A trailer system is a well-known example of flat systems. In Ref. [11], Altafini proposed a hybrid controller for the backward-motion control of a truck-and-trailer system. In Ref. [12], Lamirault and Laumond proposed the virtual-robot concept to control the backward motion of a single trailer. On the other hand, many researchers have proposed soft computing techniques for trailer control. A good example is the fuzzy controller in Ref. [13].

Mechanical and kinematic designs have been studied and some useful results have been obtained. Typical examples include the three-point trailer in Ref. [14], Bushnell's trailer Ref. [15], and Yamamiya's trailer [16].

However, it is still difficult to find practical solutions for the control problem of a robot with n passive trailers. Many of the previous studies focus on special trailer mechanisms rather than the general n trailer system. For example, the three-point trailer in Ref. [14] and Yamamiya's trailer in Ref. [16] require a somewhat complicated passive-steering mechanism. In addition, docking and releasing between trailers are not easy, which limits reconfigurability.

[†]This paper was recommended for publication in revised form by Associate Editor Kyongsu Yi

*Corresponding author. Tel.: +82 2 3290 3375, Fax.: +82 2 3290 3375
E-mail address: smartrobot@korea.ac.kr

© KSME & Springer 2011

In Ref. [17], we proposed the kinematic design of modular off-hooked passive trailers. A kinematic design was established in order to achieve high trajectory-tracking performance of passive trailers.

In this paper, it is shown how the backward motion of a robot with n passive trailers can be efficiently controlled. The problem is formulated as a trajectory-following problem, rather than as the control of independent, generalized coordinates. First, a reference trajectory of the last trailer is planned. Then, the robot pushes trailers to follow the trajectory by using a tracking controller and inverse kinematics.

In theory, there is no limitation on the number of controllable trailers. However, in practice, this number is limited. This paper provides an answer to the following question: "Does the system work well even if there exist sensing or modeling errors?" Although it is difficult to obtain general analytic solutions for the question, a practical answer will be explored through simplified analysis and experiments.

Since a multi-body trailer system is a serial chained structure, any sensing or modeling errors will affect the control performance. In practice, joint backlashes and sensing noise are possible error sources in the fabricated prototype. Therefore, it is important to investigate the effect of joint-angle errors.

Another experimental issue is to estimate lateral wheel slippage. Passive trailers and controllers are designed and controlled on the basis of kinematic analysis. This fact implies that if kinematic constraints are violated, the control performance of trailers will not be satisfactory. A basic assumption of a trailer system is that the wheels roll without slipping. A simple dynamic computation helps to predict wheel slippage.

This paper is organized as follows. Section II explains the strategy for backward-motion control. Possible error sources, including joint-angle errors and lateral wheel slippage, are investigated in Section III. Section IV presents the experimental results and discussion. Some concluding remarks are given in Section V. A part of this research was introduced in Refs. [18] and [19].

2. Backward motion control of off-hooked trailer

Fig. 1 illustrates the kinematic parameters of a robot with off-hooked trailers that was introduced in Ref. [17]. In Ref. [17], it was shown that the trajectory-tracking error can be minimized when the link length $D = F = R$. Link length D is defined as the distance between the midpoint of the trailer wheel axle and the hinge point. The lengths of front and rear links are denoted by F and R as shown in Fig. 1. It was also shown that the steady-state tracking error becomes zero when the robot moves along a curve with constant curvature.

This kinematic model is derived under the following assumptions:

- A1) The motion of the robot and trailers is 2-D planar.
- A2) Nonholonomic velocity constraints (no-side-slip) are valid at all wheels.

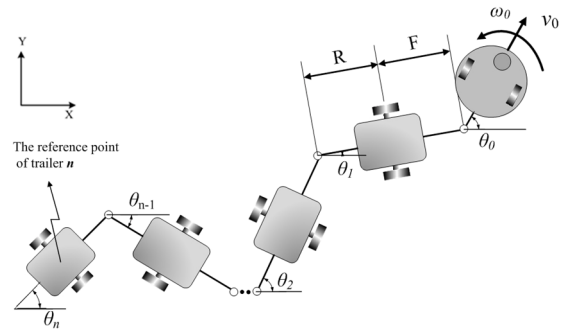


Fig. 1. Kinematic parameters of an off-hooked trailer.

A3) Dynamics can be neglected and only the kinematic model is considered.

Each trailer is equipped with passive wheels. The wheel orientations are fixed with respect to the trailers. Links are connected through free revolute joints. The proposed backward motion control scheme can be summarized as following three steps:

- Step 1) Generate the reference trajectory of the last trailer (trailer n).
- Step 2) Compute the desired motion of the last trailer $[v_n, \omega_n]^T$ from the trajectory-tracking controller.
- Step 3) Compute the control inputs, $[v_0, \omega_0]^T$, of the active robot from the kinematic model of the trailer system.

In Step 1, the desired pose, $X_d = [x_d, y_d, \theta_d]^T$, and velocity, $V_d = [v_d, \omega_d]^T$, of trailer n are planned as functions of time. The kinematic model relating the reference posture $X_d = [x_d, y_d, \theta_d]^T$ and reference motion $V_d = [v_d, \omega_d]^T$ of the last trailer can be represented by a following equation:

$$\begin{pmatrix} \dot{x}_d \\ \dot{y}_d \\ \dot{\theta}_d \end{pmatrix} = \begin{bmatrix} -\sin \theta_d & 0 \\ \cos \theta_d & 0 \\ 0 & 1 \end{bmatrix} \begin{pmatrix} v_d \\ \omega_d \end{pmatrix}. \quad (1)$$

Step 1 corresponds to the trajectory planning of the last trailer. Any existing trajectory planner for two-wheel differential robots can be adopted. For simplicity, the target trajectories are assumed to be lines and arcs with constant desired velocities.

In Step 2, the pose of trailer n converges to the target trajectory by the application of the trajectory-tracking controller. We employ Kanayama's controller given in Ref. [20]. The definition of the tracking error, $X_e = [x_e, y_e, \theta_e]^T$, for trailer n is as follows:

$$\begin{pmatrix} x_e \\ y_e \\ \theta_e \end{pmatrix} \triangleq \begin{pmatrix} \cos \theta_n & \sin \theta_n & 0 \\ -\sin \theta_n & \cos \theta_n & 0 \\ 0 & 0 & 1 \end{pmatrix} (X_d - X). \quad (2)$$

The reference point $X = [x, y, \theta]^T$ indicates the midpoint of the wheel axle of the last trailer, as shown in Fig. 1. The desired motion, $V_{ref} = [v_{ref}, \omega_{ref}]^T$, is computed from the controller as follows:

$$v_{ref} = v_d \cos \theta_e + K_x x_e \quad (3)$$

$$\omega_{ref} = \omega_d + v_d (K_y y_e + K_\theta \sin \theta_e). \quad (4)$$

The above controller is asymptotically stable and $X_e = [x_e, y_e, \theta_e]^T$ converges to zero when $V_d = [v_d, \omega_d]^T$ is continuous and bounded. In Ref. [20], Lyapunov stability was established for the linearized model. When $V_d = [v_d, \omega_d]^T$ is a constant vector, exponential stability can be achieved. The controller in Ref. [20] is widely used because of its robust control performances. As pointed out in Ref. [21], the region of asymptotic stability is quite large although its accurate determination is difficult and very few studies have explicitly addressed the robustness issue.

In Step 3, we concentrate on velocity mapping between the active robot and the last trailer. The kinematic model can be represented by the following equation:

$$\begin{aligned} \begin{pmatrix} v_0 \\ \omega_0 \end{pmatrix} &= \begin{bmatrix} \cos \psi_n & (-1)^{n-1} D \sin \psi_n \\ \sin \psi_n / D & -(-1)^{n-1} \cos \psi_n \end{bmatrix} \begin{pmatrix} v_n \\ \dot{\theta}_n \end{pmatrix} \\ \psi_i &= \sum_{k=1}^i (-1)^{k-1} (\theta_{k-1} - \theta_k), \quad i = 1, \dots, n. \end{aligned} \quad (5)$$

An active robot is holonomic and omni-directional. Therefore, two velocity inputs, viz., $[v_0, \omega_0]^T$, can be arbitrarily specified. In addition, it is assumed that the input velocities are accurately controlled. From Eq. (5), it is clear that singularity occurs when $D = 0$. More specifically, $F = 0$ and $R = 0$ are the singularity conditions when the robot moves forward and backward, respectively. The off-hooked trailer is advantageous because a direct mapping always exists between the input velocities, $[v_0, \omega_0]^T$, and the velocities of the last trailer $[v_n, \omega_n]^T$. This fact implies that the last trailer can be considered as an active robot because it can be actively controlled at any time.

From the viewpoint of kinematics, the problem of backward-motion control is completely identical to the control of the forward motion when the rest of the bodies are towed by the last trailer. Since the off-hooked trailer shows superior performance in trajectory tracking, the control problem becomes extremely simple. Any existing controllers for two-wheeled differential robots can be adopted in order to control the last trailer. The joint angles are monitored online and the pose of the pushing robot is obtained by localization.

3. Error sources of backward motion control

3.1 Joint-angle errors

In practice, the control performance is affected by various

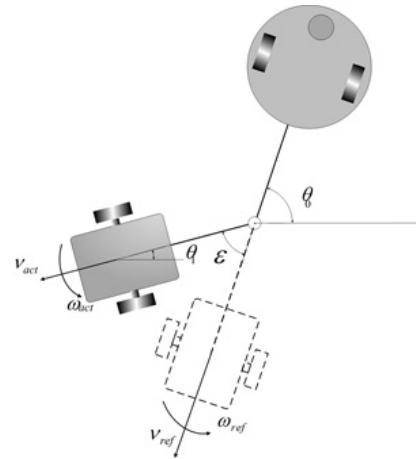


Fig. 2. A mobile robot with a trailer under the joint-angle measurement error, ϵ .

error sources. As pointed out in Ref. [21], control robustness with respect to uncertainties and disturbances is an open and challenging issue in nonholonomic system control. Although it is difficult to analyze the properties of general backward motion control, it is possible to investigate the effect of errors for a specific case. For simplicity, the following assumptions are made:

- B1) The reference trajectory is a straight line along the x -axis.
- B2) A robot with one trailer is considered.
- B3) The local configuration around $\theta \approx 0$, $\theta_e \approx 0$ is considered.
- B4) The translational velocity is perfectly controlled ($x_e \approx 0$).

We concentrate on measurement errors for joint angles. In the fabricated prototype, the errors in joint-angle measurement can be assumed to be constants because of the difficulty of wheel alignment across multiple trailers. Since the structure of trailers is a serial chain, joint-angle errors directly affect the control performance. In Ref. [22], Chung established the sensitivity to errors of a serial-chained system under nonholonomic constraints. It is advantageous to mechanically allow relative motion between trailers to cope with uneven ground conditions. Otherwise, some trailers possibly encounter “wheel floating” under irregular ground conditions, as pointed out by Nakamura et al. in Ref. [14]. The relative motion between trailers may result in joint-angle measurement errors.

Since the backward motion is feedback controlled by using the scheme proposed in Section 2, some errors can be compensated. The above assumptions, B3 and B4, become feasible owing to the robustness of the feedback controller. Fig. 2 shows a robot with one trailer in backward-motion control. The solid line shows the actual configuration. The dashed line represents the configuration that contains the joint-angle measurement error, ϵ . The reference velocities of the trailer,

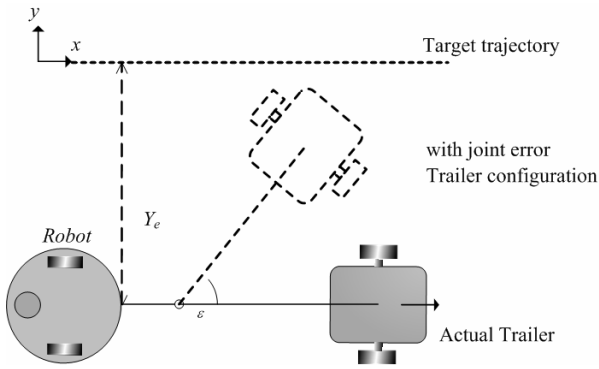


Fig. 3. The robot pushes the trailer to the right under the joint-angle measurement error, ε . The robot moves straight with the steady-state error, Y_e .

$[v_{ref}, \omega_{ref}]^T$, are computed from the trajectory-tracking controller. The control input of the robot, $[v_0, \omega_0]^T$, is determined using Eq. (5). The measurement error, ε , is included as follows:

$$\begin{pmatrix} v_0 \\ \omega_0 \end{pmatrix} = \begin{bmatrix} \cos(\theta_0 - \theta_1 - \varepsilon) & D\sin(\theta_0 - \theta_1 - \varepsilon) \\ \sin(\theta_0 - \theta_1 - \varepsilon)/D & -\cos(\theta_0 - \theta_1 - \varepsilon) \end{bmatrix} \begin{pmatrix} v_{ref} \\ \omega_{ref} \end{pmatrix}. \quad (6)$$

Then, the resultant velocity of the real trailer, $[v_{act}, \omega_{act}]^T$, can be obtained as follows:

$$\begin{aligned} \begin{pmatrix} v_{act} \\ \omega_{act} \end{pmatrix} &= \begin{bmatrix} \cos(\theta_0 - \theta_1) & D\sin(\theta_0 - \theta_1) \\ \sin(\theta_0 - \theta_1)/D & -\cos(\theta_0 - \theta_1) \end{bmatrix} \begin{pmatrix} v_0 \\ \omega_0 \end{pmatrix} \\ &= \begin{bmatrix} \cos \varepsilon & -D\sin \varepsilon \\ \sin \varepsilon/D & \cos \varepsilon \end{bmatrix} \begin{pmatrix} v_{ref} \\ \omega_{ref} \end{pmatrix}. \end{aligned} \quad (7)$$

From Eq. (7), we can find the relationship between the reference and actual velocities under joint-angle errors. It is clear that $[v_{act}, \omega_{act}]^T = [v_{ref}, \omega_{ref}]^T$, when $\varepsilon = 0$.

From Eq. (4), it is clear that $\omega_{ref} = 0$ when there is no tracking error. If there is no joint-angle measurement error, then Eq. (7) implies that $\omega_{act} = 0$. Accordingly, the robot and the trailer head in a constant direction by following a straight line. Similarly, we assume the configuration that results in $\omega_{act} = 0$ under the joint-angle measurement error. Fig. 3 shows this assumption when the target trajectory is $y = 0$ and the robot is moving to the right.

From Eq. (7), the following condition is derived when $\omega_{act} = 0$.

$$\frac{\omega_{ref}}{v_{ref}} = -\frac{1}{D} \tan \varepsilon \quad (8)$$

From Eqs. (2)-(4), (8), and assumption B4, the steady-state error, Y_e , can be obtained through a following equation:

$$Y_e = -\frac{1}{D \cdot K_y} \tan \varepsilon. \quad (9)$$

The above condition provides an equilibrium point of convergence. In addition, it can be easily checked that the equilibrium point is stable. For example, if $y_e < Y_e$ ($y_e > Y_e$), y_e increases (decreases) to Y_e because ω_{act} is positive (negative). Therefore, we can conclude that the trailer locally converges to a straight line with the steady-state error, Y_e , if there is joint-angle measurement error, ε . It is assumed that ε is small ($\varepsilon \approx 0$). This result can be iteratively extended to the n -trailer problem. It is assumed that the resultant tracking error is the sum of the individual tracking errors when there are multiple joint-angle errors.

Since the equilibrium point can be obtained as in Eq. (9), it is necessary to investigate the control stability of backward-motion control with joint-angle errors. In Ref. [20], the asymptotic stability of the tracking controller was shown for a conventional, two-wheeled robot. We investigate the stability condition for the kinematic model in Eq. (7). The following equation is obtained by combining Eqs. (3), (4), and (7):

$$\begin{pmatrix} \dot{x}_e \\ \dot{y}_e \\ \dot{\theta}_e \end{pmatrix} = \begin{pmatrix} \omega_{act} \cdot y_e - v_{act} + v_r \cdot \cos \theta_e \\ -\omega_{act} \cdot x_e + v_r \cdot \sin \theta_e \\ \omega_r - \omega_{act} \end{pmatrix}. \quad (10)$$

The above equation can be linearized by adopting the assumptions from B1 through to B4 as in the following equation:

$$\dot{\mathbf{X}}_e = \mathbf{A}\mathbf{X}_e. \quad (11)$$

In Eq. (10),

$$\mathbf{A} = \begin{pmatrix} -K_x & v_d \cdot K_y \cdot D \cdot \varepsilon & K_\theta \cdot D \cdot \varepsilon \\ 0 & 0 & v_d \\ 0 & -v_d \cdot K_y & -v_d \cdot K_\theta \end{pmatrix}. \quad (12)$$

The characteristic equation of the matrix, \mathbf{A} , can be derived as the following equation:

$$\begin{aligned} s^3 + (v_d K_\theta + K_x)s^2 + (v_d^2 K_y + v_d K_x K_\theta)s + v_d^2 K_x K_y \\ = a_1 s^3 + a_2 s^2 + a_3 s + a_4 = 0. \end{aligned} \quad (13)$$

All coefficients, $\{a_i\}$, are positive and $a_2 a_3 - a_1 a_4 > 0$, the real parts of all roots are negative from the Routh-Hurwitz Criterion. Therefore, the linearized system in Eq. (11) is proven to be asymptotically stable. Ref. [20] gives more details about the proof of asymptotic stability.

3.2 Lateral slippage of trailers

From the viewpoints of kinematics and control theory, there is no limitation on the number of controllable trailers. However, it is worth investigating the dynamic limitation on the available number of trailers for practical applications. The focus of dynamic analysis is to estimate the violation of kine-

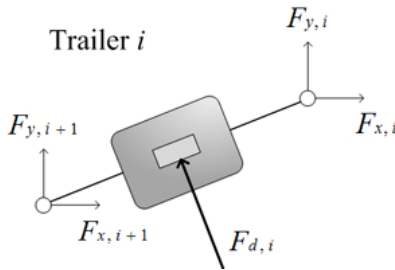


Fig. 4. Definition of the external forces and force equilibrium of trailer i .

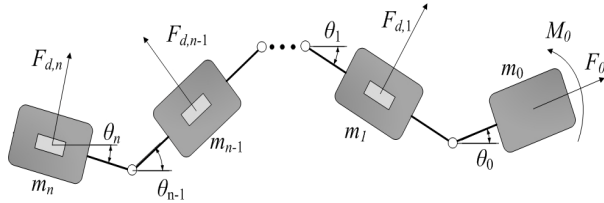


Fig. 5. External forces of the robot with an n -trailer system.

matic constraints. The kinematic model in Eq. (5) was derived under the assumption that wheels roll without lateral slippage. The kinematic constraints are violated when the lateral force exceeds the maximum frictional force. In order to compute the lateral forces at the trailer wheels, a simple dynamic computation is carried out.

It is difficult to accurately estimate wheel slippage because of various floor conditions and the nonlinearity of the tire model. In order to arrive at an approximate estimate, the following assumptions are made:

- C1) The passive wheel axles and hinges between neighboring trailers are free joints.
- C2) The two parallel wheels of each trailer are modeled by a single wheel at the center of the wheel axle.
- C3) Coulomb friction is assumed between the wheels and the ground.
- C4) The robot “slowly” moves to avoid large dynamic forces. The robot velocities are accurately controlled.

Fig. 4 shows the force equilibrium of the simplified model for trailer i . The mass and moment of inertia of trailer i are m_i and I_i , respectively. $F_{x,i}$, $F_{y,i}$, $F_{x,i+1}$, and $F_{y,i+1}$ correspond to the internal forces when trailers $i+1$ and $i+2$ are interconnected with trailer i . For simplicity, it is assumed that the mass center of a trailer is located at the midpoint of the wheel axle.

Since the robot is holonomic and omni-directional, the input force and torque can be arbitrary specified as F_0 and M_0 , respectively. Fig. 5 shows the external forces of the robot with n trailers. Owing to assumption C4, all velocities and accelerations can be computed using Eq. (5) when the robot’s motion is determined. Fig. 6 shows the definition of the position vec-

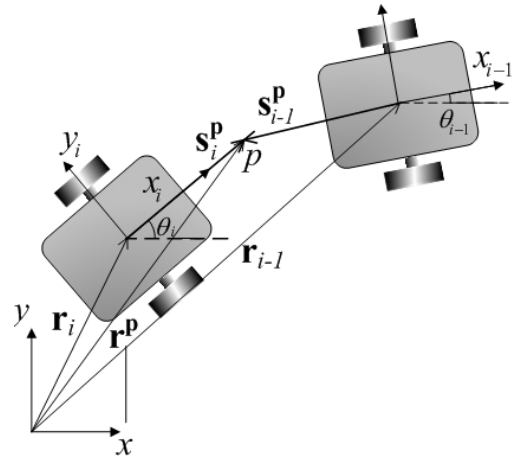


Fig. 6. Definition of the position vectors.

tors. We can derive the lateral force, $F_{d,i}$, of the i^{th} trailer as in the following equation:

$$\begin{aligned} F_{d,i} = & -I_i \ddot{\theta}_i / d - \{2 \cos(\theta_i - \theta_{i+1}) F_{d,i+1} \\ & + 2 \cos(\theta_i - \theta_{i+2}) F_{d,i+2} + \dots + 2 \cos(\theta_i - \theta_n) F_{d,n} \\ & + \sin \theta_i (m_i \ddot{x}_i + 2m_{i+1} \ddot{x}_{i+1} + 2m_{i+2} \ddot{x}_{i+2} + \dots + 2m_n \ddot{x}_n) \\ & - \cos \theta_i (m_i \ddot{y}_i + 2m_{i+1} \ddot{y}_{i+1} + 2m_{i+2} \ddot{y}_{i+2} + \dots + 2m_n \ddot{y}_n)\}. \end{aligned} \quad (14)$$

In Eq. (14), \ddot{x}_i , \ddot{y}_i are the accelerations of the i^{th} trailer. The kinematic constraints are derived as follows:

$$\begin{aligned} 0 = & \mathbf{r}_{i-1} + \mathbf{A}_{i-1} \mathbf{s}_{i-1}^p - \mathbf{r}_i - \mathbf{A}_i \mathbf{s}_i^p \\ 0 = & \ddot{\mathbf{r}}_{i-1} + \ddot{\theta}_{i-1} \mathbf{B}_{i-1} \mathbf{s}_{i-1}^p - \dot{\theta}_{i-1}^2 \mathbf{A}_{i-1} \mathbf{s}_{i-1}^p - \ddot{\mathbf{r}}_i - \ddot{\theta}_i \mathbf{B}_i \mathbf{s}_i^p + \dot{\theta}_i^2 \mathbf{A}_i \mathbf{s}_i^p. \end{aligned} \quad (15)$$

In Eq. (14), \mathbf{s}_i^p is the local position vector of point p on trailer i ,

$$\mathbf{A}_i = \begin{bmatrix} \cos \theta_i & -\sin \theta_i \\ \sin \theta_i & \cos \theta_i \end{bmatrix} \quad (16)$$

$$\mathbf{B}_i = \begin{bmatrix} -\sin \theta_i & -\cos \theta_i \\ \cos \theta_i & -\sin \theta_i \end{bmatrix}. \quad (17)$$

It is noteworthy that $F_{d,i}$ is dependent upon lateral forces and accelerations of “outer” trailers from trailer $i+1$ to trailer n in Eq. (14). For trailer i in Fig. 4, three equations can be obtained by Newton-Euler equations in terms of five external forces and three inertial forces. Since the motion of trailers is given, inertial forces are known. For trailer n , three external forces can be solved by three equations. For every “inner” trailer, three unknown forces are iteratively added. The unknowns can be solved from additional three equations.

The mass and maximum friction of the fabricated prototype can be easily obtained experimentally. If $F_{d,i}$ in Eq. (14) exceeds the maximum friction force, $F_{f,i}$, lateral slippage takes



Fig. 7. The experimental prototype of a mobile robot with three passive trailers.



Fig. 8. A passive off-hooked trailer (left) and a docking mechanism (right).

place at the i^{th} trailer. This slippage can be avoided by reducing the acceleration of the trailer system by changing the inputs.

4. Experiment

4.1 Prototype

Fig. 7 shows a prototype of the trailer system. The PSR2 is a holonomic, omni-directional mobile robot. For backward-motion control, a laser range finder is installed at the last trailer and points backward.

Fig. 8 shows a prototype of a passive trailer. The link length, D , in Eq. (4) is 0.52 m. Each trailer has two passive wheels with fixed orientations and two casters. The kingpin is designed for the docking and releasing of trailers. The joint angles are measured by potentiometers at each joint. Each trailer is equipped with brake systems in order to prevent rolling when the trailer is separated from the robot.

4.2 Backward-motion control

Experimental verifications are carried out for two reference trajectories, which are a straight line and a circle, respectively. The PSR2 computes the current position of the robot by using laser scanners. The trailer positions are computed from the potentiometer measurements and link parameters.

Fig. 9 shows the result of backward-motion control when the system is driven along the center of the corridor. Since the backward motion of the trailer system is open loop unstable, the robot becomes zigzag without the proposed controller. The details of the open loop motion are presented in Ref. [17]. In



(a)

(b)



(c)

(d)



(e)

(f)

Fig. 9. Backward motion of a robot with three trailers for a straight reference trajectory. The impulse disturbance is given at (b).

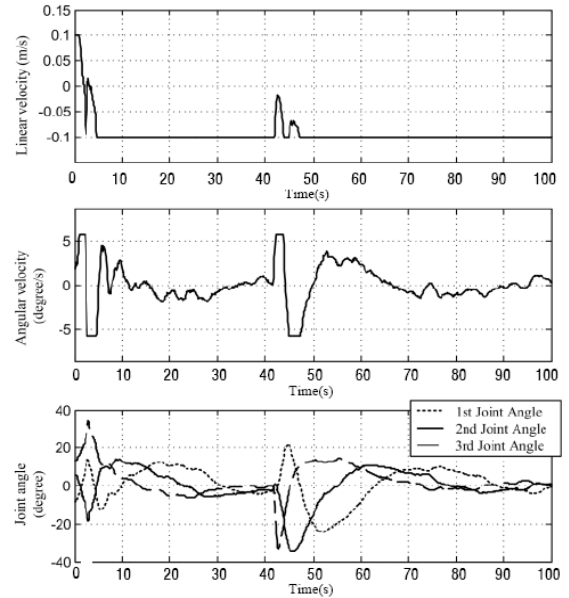


Fig. 10. The two input velocities, $[v_0, \omega_0]^T$, of the robot and the joint angles for the straight reference trajectory.

order to investigate the disturbance-rejection performance, the last trailer was intentionally pushed to the right, as shown in Fig. 9(b). It is clear that the tracking error is compensated, as shown in Fig. 9(d) and Fig. 9(e). Finally, the system successfully recovered the desired trajectory, as depicted in Fig. 9(f). Fig. 10 shows the two input velocities $[v_0, \omega_0]^T$ of the robot and joint angles. The maximum speeds of the robot were lim-

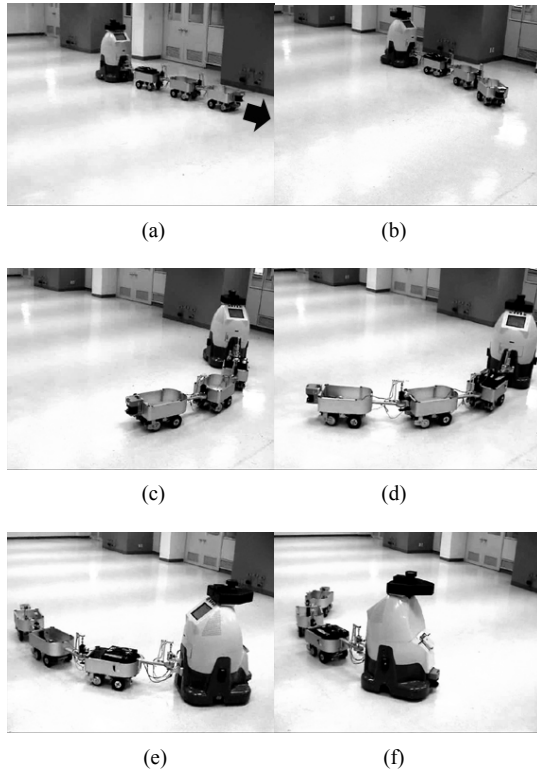


Fig. 11 Backward motion of a robot with 3 trailers for a circular reference trajectory.

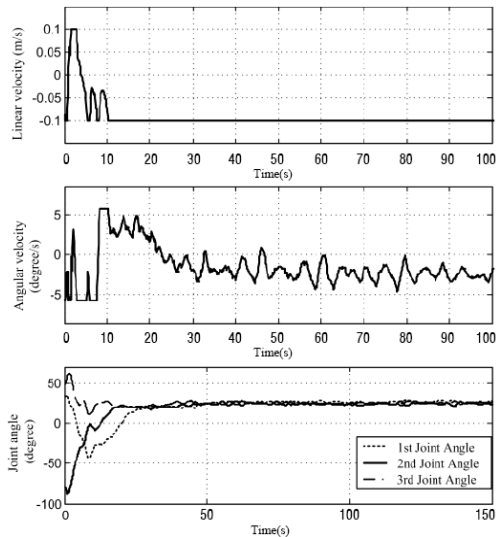


Fig. 12. The experimental values of the two input velocities, $[v_0, \omega_0]^T$, and the joint angles of the robot for the circular reference trajectory.

ited to 0.1 m/s and 0.1 rad/s. The input velocities show small changes around $t = 40$ to 50 s, due to the impulse disturbance. Since the reference trajectory is straight, the steady-state joint angles are zero. From Fig. 10, it is evident that the joint angles converge to zero.

Fig. 11 shows the experimental motion when the reference trajectory is a circle. The radius of the reference circle is 2.5 m.

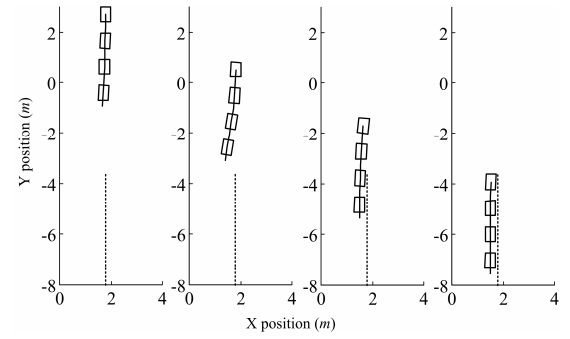


Fig. 13. Steady-state error of tracking control in backward motion under the joint error of $\epsilon = 5^\circ$.

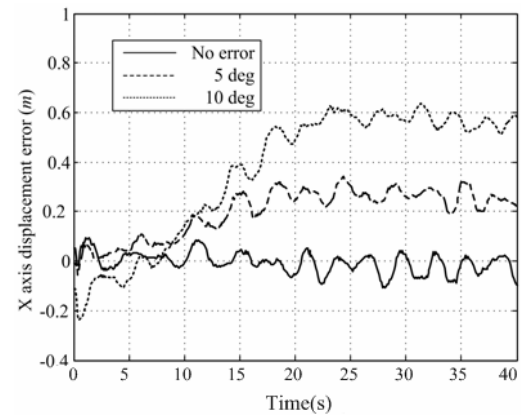


Fig. 14. Steady-state error of the last trailer under different joint errors.

If the trailer system converges to the path, then the joint angles should converge to 25° . Fig. 12 shows the two inputs $[v_0, \omega_0]^T$ and the joint angles. After convergence at around 20 s, the trailers accurately followed the target trajectory. The steady-state error of the joint angle was about 23° . The trajectory-tracking error was always smaller than 0.2 m. Possible error sources are the joint angle measurement error, backlashes at joints, uneven floor, and so forth.

From the experimental results, it was shown that the backward motion of trailers could be easily controlled. For example, a target trajectory of the last trailer can be easily generated by using Reeds & Shepp's approach, which was presented in Ref. [23]. Since the trajectory is composed of circles and lines, the trailers easily can be controlled by using the proposed scheme.

4.3 The effect of joint angle errors

Section III-A discussed the effect of joint measurement errors. In order to investigate the effect of the joint error, a constant error, ϵ , is intentionally added to the measured joint angle of the third trailer. In experiments, three values of ϵ were tested: 0° ; 5° ; and 10° .

Fig. 13 shows the robot's trajectory for $\epsilon = 5^\circ$. The trailer system follows the reference path with an offset distance. The

Table 1. Parameters of simulations and experiments.

Trailers' specifications	
Mass	42.1 kg
Link length	0.52 m
Dimension	0.6m * 0.8 m
Friction coefficient	0.09
Sampling time	0.005 s

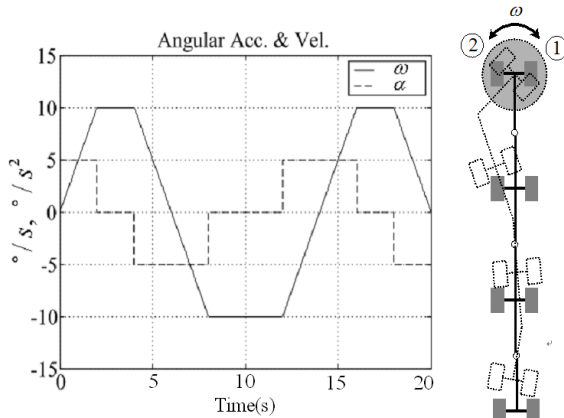


Fig. 15. Input angular velocity and angular acceleration of the robot (left) and configurations of the trailer system.

steady-state error is a balanced configuration between the effect of the joint measurement error in Eq. (6) and the effect of the closed-loop controller in Eq. (3).

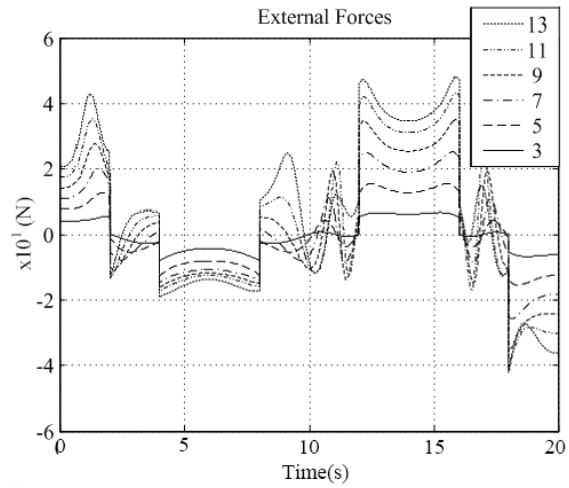
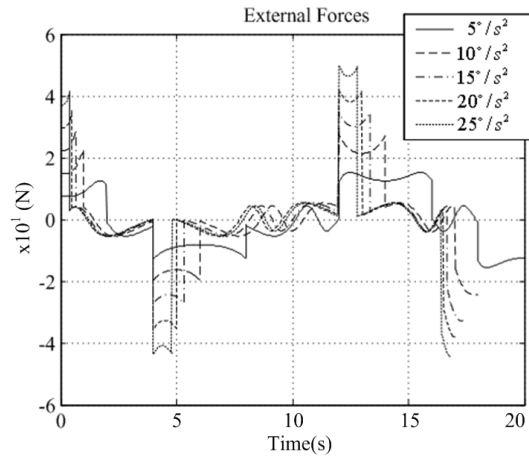
Fig. 14 shows the steady-state tracking error of the three experiments. It can be seen that the tracking error increases with ε . This result coincides with the analysis in Eq. (8). Following convergence, there are small oscillations due to joint backlashes but the oscillations are acceptably small.

From the experimental results, we can conclude that the backward motion of trailers can be successfully controlled even though there are joint errors. The accumulation of errors results not in a lack of stability of control but in steady-state errors. On the other hand, joint measurement errors can be experimentally calibrated by monitoring the steady-state error.

4.4 Estimation of wheel slippage through dynamic simulations

Simulations are carried out in order to investigate dynamic effects. The simulation parameters are determined on the basis of the prototype, as shown in Table 1. Since the wheel slippage takes places instantaneously, the detection of slippage is difficult in practice. Therefore, experiments are carried out without translational motion. The robot makes a periodic pure rotating motion, as shown in Fig. 15.

The initial robot configuration is ①, as shown in the right of Fig. 15. Then, the configuration reaches ② at around 6 s. Fig. 15 shows the angular velocity and the angular accelera-

Fig. 16. Variation of the lateral force of the first trailer, $F_{d,1}$, with the number of passive trailers.Fig. 17. The variation of $F_{d,1}$ with the increase of input angular acceleration α of the robot.

tion of the robot. From simulations, we found out that $F_{d,i}$ in Eq. (13) is always the largest at the first trailer ($i = 1$). This fact implies that the lateral wheel slippage of the first trailer takes place first. Therefore, we concentrate on the lateral slippage of the first trailer in simulations and experiments. The experimental static frictional force of lateral slippage was approximately 37.2 N, as shown in Table 1. Therefore, $0F_{d,i} < 37.2N$ for $\forall i$ should be satisfied in order to guarantee that wheels roll without lateral slippage.

Fig. 16 shows the variation of the lateral force of the first trailer, $F_{d,1}$, when the number of trailers increases. It is clear that the external force on the first trailer-wheel increases when the number of trailers increases. When there are nine or more trailers, $F_{d,1}$ exceeds the upper limit on the static frictional force. At that moment, lateral wheel slippage takes place. Therefore, it can be concluded that seven or less trailers can be safely controlled without violating kinematic constraints under the present experimental conditions. The number of controlla-

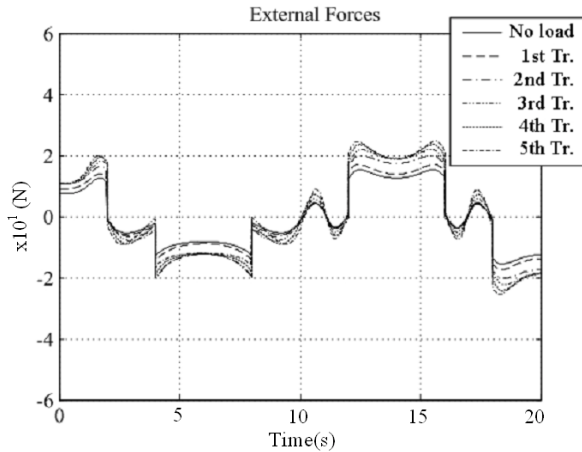


Fig. 18. The variation of $F_{d,l}$ when an 80kg weight is loaded on the i^{th} trailer.

ble trailers is limited by the dynamic properties even though there is no limitation from the viewpoint of kinematics and control theory.

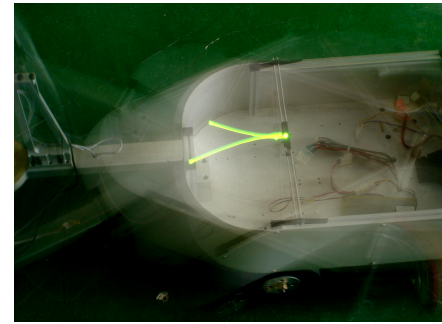
Fig. 17 shows the simulation results when the input angular acceleration, α , increases. It is evident that $F_{d,l}$ increases with α . In Fig. 17, it can be seen that $F_{d,l}$ exceeds the maximum static frictional force (37.2 N) when $\alpha > 15^{\circ}/s^2$. In other words, the three trailer system can be safely controlled when $\alpha \leq 10^{\circ}/s^2$. It must be noted that the motion in Fig. 15 can be safely controlled because $|\alpha| \leq 5^{\circ}/s^2$. This result implies that the possibility of wheel slippage can be reduced by decreasing the acceleration of the robot. In practical applications, control inputs can be modulated using online dynamic computations in order to reduce $F_{d,l}$.

We investigate the effect of loading conditions. An 80kg-weight was loaded on to one trailer. Fig. 18 shows the variation of $F_{d,l}$ when the weight is loaded on to the i^{th} trailer. It can be seen that $F_{d,l}$ is maximum when the weight is loaded on the last trailer. This result shows that the possibility of lateral slippage becomes high when the last trailer is heavily loaded. Therefore, it is recommended that heavy objects be loaded in the foregoing trailers.

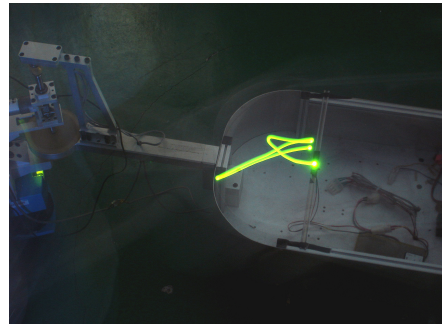
4.5 Experiments with the prototype of a robot with three trailers

Experiments were carried out with the prototype of the robot with three trailers. The experimental conditions were identical to those in Table 1. In order to visualize wheel slippage, we took pictures with long exposure times during the robotic motion. A green LED was installed at the center of the first trailer. The LED showed the movement of the first trailer when the robot was driven by the inputs depicted in Fig. 15.

Fig. 19(a) shows that the locus of the LED exhibited a cusp when there was no lateral slippage. Fig. 19(b) shows that momentary slippage took place when $\omega = 20^{\circ}/s$ and $\alpha = 30^{\circ}/s^2$. This result coincides with the result in Fig. 17. Fig. 17 shows that lateral wheel slippage can take place when $\alpha > 15^{\circ}/s^2$.



(a) No slippage, pure rolling when $|\alpha| \leq 5^{\circ}/s^2$



(b) Momentary slippage when $|\alpha| \leq 20^{\circ}/s^2$



(c) Complete slippage when $|\alpha| \leq 30^{\circ}/s^2$

Fig. 19. Wheel slippage experiments. The resultant paths were visualized by the LED locus.

Fig. 19(c) shows the motion when $\omega = 40^{\circ}/s$ and $\alpha = 50^{\circ}/s^2$. In addition, a 50 kg weight was loaded on to the last trailer to create a severe condition. As shown in Fig. 19(c), the trailer was out of control due to complete slippage throughout the motion. We can conclude that kinematic constraints were violated and that the kinematic model in Eq. (5) is inapplicable. The experimental results showed that the simple dynamic analysis outlined in section III-B is useful to estimate wheel slippage. From the results of simulations and experiments, it is clear that trailer systems should be carefully controlled by taking into account dynamic characteristics.

5. Conclusion

We have proposed a scheme for the backward-motion con-

trol of a passive multiple-trailer system. The effect of the joint-angle measurement error was investigated. A simple dynamic analysis was presented and the usefulness was verified through simulations and experiments.

Since the proposed controller is developed for general multi-axle trailer systems, it can be applied to similar systems. For example, a kinematic model of a car-like vehicle corresponds to a mobile robot with one trailer. Therefore, the control inputs of such systems can be obtained by the appropriate coordinate and input transformations.

In practical multiple-trailer systems, the consideration of dynamics is important. Although there have been many studies on trailer systems, it is difficult to find useful experimental results for general n trailers. By exploiting the proposed strategies, trailer systems can be successfully controlled without violating kinematic constraints.

Acknowledgment

This work was supported in part by the MKE under the Human Resources Development Program for Convergence Robot Specialists. This work was also supported in part by the NRF grant funded by the MEST (2011-0016225). This work was also supported in part by Basic Science Research Program through the NRF funded by the MEST (2010-0022609). This work was also supported in part by the MKE under the ITRC support program.

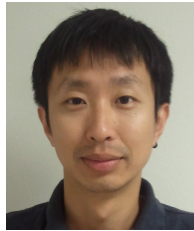
References

- [1] W. Chung, G. Kim and M. Kim, Development of the multi-functional indoor service robot PSR systems, *Autonomous Robots*, 22 (1) (2007) 1-17.
- [2] J. Kang, W. Kim, J. Lee and K. Yi, Design, implementation, and test of skid steering-based autonomous driving controller for a robotic vehicle with articulated suspension, *The Journal of Mechanical Science and Technology*, 24 (3) (2010) 793-800.
- [3] J. -H. Seo, Analysis and design study of LCD transfer robot using dynamic simulation and experiment, *The Journal of Mechanical Science and Technology*, 23 (4) (2009) 1035-1039.
- [4] S. Lee, Use of coded infrared light for mobile robot localization, *The Journal of Mechanical Science and Technology*, 22 (7) (2008) 1279-1286.
- [5] W. Li, T. Tsubouchi and S. Yuta, Manipulative difficulty index of a mobile robot with multiple trailers in pushing and towing with imperfect measurement, *Proc. of the 2000 IEEE International Conference on Robotics and Automation*, C.A. April, 2000.
- [6] J. P. Laumond, Controllability of a multibody mobile robot, *IEEE Transactions on Robotics and Automation*, 9 (6) (1993).
- [7] R. M. Murray and S. S. Sastry, Nonholonomic motion planning: steering using sinusoids, *IEEE Transactions on Automatic Control*, 38 (5) (1993) 700-716.
- [8] D. M. Tilbury, R. M. Murray and S. S. Sastry, Trajectory generation for n-trailer problem using Goursat normal form, *Proceedings of the IEEE control and Decision conference* (1993) 971-977.
- [9] O. J. Sørdalen and K. Y. Wichlund, Exponential stabilization of a car with n trailers, *Proceeding of 32nd conference on Decision and Control*, San Antonio (1993) 978-983.
- [10] P. Rouchon, M. Fliess, J. Levine and P. Martin, Flatness, motion planning and trailer systems, *Proceedings of the 32th IEEE Conf. on Decision and Control*, , San Antonio, Texas (1993) 2700-2705.
- [11] C. Altafini, Some properties of the general n-trailer, *International Journal of Control*, 74 (4) (2001) 409-424.
- [12] F. Lamiraux and J. P. Laumond, A practical approach ro feedback control for a mobile robot with trailer, *Proceedings of the 1998 International Conference on Intelligent Robotics and Automation*, Leuven, Belgium (1998) 3291-3296.
- [13] K. Tanaka, S. Hori and H. O. Wang, Multiobjective control of a vehicle with triple trailers, *IEEE/ASME Transactions on mechatronics*, 7 (3) (2002) 357-368.
- [14] Y. Nakamura, H. Ezaki and W. Chung, Design of steering mechanism and control of nonholonomic trailer system, *IEEE transactions on Robotics and Automation*, 17 (3) (2001) 367-374.
- [15] L. Bushnell, Off-tracking bounds for a car pulling trailers with king pin hitching, *Proc. of the 1994 IEEE International Conference on Decision and Control*, F.L., December, 1994.
- [16] K. Yamamia, Japan patent office, *Trailer* (in Japanese), B62D13-00 H2-18 928, 1990.
- [17] J. Lee, W. Chung, M. Kim and J. Song, A passive multiple trailer system with off-axle hitching, *International Journal of Control, Automation and Systems*. 2 (3) (2004) 289-297.
- [18] M. Park, W. Chung and M. Kim, Experimental research of a passive multiple trailer system for backward motion control, *In Proceedings 2005 IEEE International Conference on Robotics and Automation*, Barcelona, April 2005, 106-111.
- [19] M. Park, W. Chung, M. Kim and J. Song, Control of a mobile robot with passive multiple trailers, *In Proc. 2004 IEEE International Conference on Robotics and Automation*, New Orleans, April 2004, 4369-4374.
- [20] Y. Kanayama, Y. Kimura, F. Miyazaki and T. Noguchi, A stable tracking control method for a non-holonomic mobile robot, *IEEE/RSJ International Workshop on intelligent Robots and Systems IROS '91*, Osaka, Japan, 1991, 1236-1241.
- [21] J. -P. Laumond, *Robot Motion Planning and Control*, Springer Verlag, 1998.
- [22] W. Chung and Y. Nakamura, Design and control of a chained form manipulator, *The International Journal of Robotics Research*, 21 (5-6) (2002) 389-408.
- [23] J. A. Reeds and L. A. Shepp, Optimal paths for a car that goes both forwards and backwards, *Pacific Journal of Mathematics*, 145 (2) (1990).

- [24] M. Vidyasagar, *Nonlinear Systems Analysis*, 1st edition. Prentice-Hall Inc. Englewood Cliffs, N.J., 1978.



Woojin Chung received the B.S. degree from the Department of Mechanical Design and Production Engineering, Seoul National University, Seoul, Korea, in 1993 and the M.S. and Ph.D degrees from the Department of Mechano-Informatics, The University of Tokyo, Tokyo, Japan, in 1995 and 1998, respectively. From 1998 to 2005, he was a Senior Research Scientist with the Korea Institute of Science and Technology. Since 2005, he has been with the Department of Mechanical Engineering, Korea University, Seoul. His research interests include the design and control of nonholonomic underactuated mechanical systems, trailer system design and control, and mobile robot navigation. Dr. Chung received an Excellent Paper Award from the Robotics Society of Japan in 1996 and the King-sun Fu Memorial Best Transactions Paper Award from the IEEE Robotics and Automation Society in 2002.



Myoungkuk Park received B.S. degree in Mechanical Engineering from Kyunghee University in 2002 and M.S. degree in Mechanical Engineering from Korea University in 2004. He is currently a graduate student pursuing Ph.D degree of mechanical engineering department at Texas A&M university, U.S..

His research interests are control systems, robotics, optimal controls and large scale stochastic dynamic programs.



Kwanghyun Yoo received B.S. and M.S. from the Department of Mechanical Engineering, Korea University, Seoul, Korea, in 2008 and 2010, respectively. In 2010, he joined the Hyundai Steel Company as a Technical Research Personnel. His research interests are mobile robot navigation and localization, trailer system design and control.



Jae Il Roh received B.S. and M.S from Department of Mechanical Engineering, Korea University, Seoul, Korea, in 2009 and 2011, respectively. In 2011, he joined the INUS Technology as a Technical Research Personnel. His research interests are mobile robot navigation and localization, trailer system control.



Jongsuk Choi received B.S., M.S., and Ph.D in Electrical Engineering from the Korea Advanced Institute of Science and Technology in 1994, 1996, and 2001. In 2001, he joined the Intelligent Robotics Research Center, Korea Institute of Science and Technology (KIST), Seoul Korea as a Research Scientist, and now is a Principal Research Scientist at Bio-medical Research Institute, KIST. His research interests include signal processing, human-robot interaction, mobile robot navigation and localization.